International Journal of Concrete Structures and Materials
DOI 10.1186/s40069-018-0249-4
ISSN 1976-0485 / eISSN 2234-1315

Bond Behavior of Pretensioned Strand Embedded in Ultra-High-Performance Fiber-Reinforced Concrete

Hyun-Oh Shin[1,2], Seung-Jung Lee[2], and Doo-Yeol Yoo[3],*

(Received June 24, 2017, Accepted January 16, 2018)

Abstract: This study aimed to investigate the bond properties of prestressing strands embedded in ultra-high-performance fiber-reinforced concrete (UHPFRC). Toward this end, two types of prestressing strands with diameters of 12.7 and 15.2 mm were considered, along with various concrete cover depths and initial prestressing force magnitudes. The average bond strength of the strands in UHPFRC was estimated by using pullout tests, and the transfer length was evaluated based on a 95% average maximum strain method. Test results indicated that the average bond strength of the pretensioned strand reduced as the diameter of the strand increased, and was between the bond strengths of round and deformed steel rebars. Higher bond strength was also obtained with a lower embedment length. Based on a comparison of p value, the bar diameter and embedment length most significantly influenced the bond strength of strands in UHPFRC, compared to a ratio of cover depth to diameter and initial prestressing force. Pretensioned strands in UHPFRC exhibited much higher bond strength and shorter transfer length compared with strands embedded in ordinary high-strength concrete. Lastly, ACI 318 and AASHTO LRFD codes significantly overestimated the transfer length of the strands embedded in UHPFRC.

Keywords: ultra-high-performance fiber-reinforced concrete, prestressing strand, bond strength, transfer length.

1. Introduction

Superior tensile performance (over 8 MPa) and durability of ultra-high-performance fiber-reinforced concrete (UHPFRC) compared with ordinary concrete make it ideal for applications in bridge girders and decks (Richard and Cheyrezy 1995; Yoo et al. 2014a, 2016a). For these applications, the load transfer mechanism between UHPFRC and the steel reinforcement, which is characterized by bonding action, is a crucial factor determining efficiency of the composite behavior of the members.

Previous studies (Jungwirth and Muttoni 2004; Holschemacher et al. 2004; Sayed Ahmad et al. 2011; Yoo et al. 2014a, b, 2015; Yuan and Graybeal 2015; Yoo and Yoon 2016, 2017) established bond characteristics between UHPFRC and reinforcing bars, such as deformed and round steel reinforcing bars, and fiber-reinforced polymer (FRP) bars. Based on previous studies, the bond strength of the steel reinforcing bars embedded in UHPFRC was significantly higher, approximately 5–10 times, than that of steel bars in ordinary concrete. It was also concluded that the bond strength between steel reinforcing bars and UHPFRC was insignificantly affected by the fiber content, but was clearly correlated with the compressive strength and side cover depth; the bond strength increased with increasing side cover and compressive strength of UHPFRC (Yuan and Graybeal 2015; Yoo and Yoon 2016). However, the bond strength slightly decreased with increasing bar diameter and embedment length owing to the nonlinear distribution of the bond stress and the Poisson's ratio effect (Yoo et al. 2015). For the FRP bars, especially glass-fiber-reinforced polymer bars embedded in UHPFRC, the bond strength was about 70% lower than that of steel reinforcing bars (Yoo and Yoon 2017). The bond failure of the FRP bars in UHPFRC was characterized by the delamination of the resin and fiber in the bar (Sayed Ahmad et al. 2011; Yoo and Yoon 2016). Previous studies also proposed analytical models for predicting the bond strengths of steel reinforcing bars and FRP bars embedded in UHPFRC.

On the other hand, studies on the bond behavior between UHPFRC and prestressing strands is very limited, although most bridge girders and decks made of UHPFRC are pretensioned members. Heffer et al. (2004) investigated the minimum concrete cover and the minimum clear spacing between the strands necessary for the anchorage zone of pretensioned members with UHPFRC and a seven-wire

[1)]Department of Agricultural and Rural Engineering, Chungnam National University, 99 Deahak-ro, Yuseong-gu, Daejeon 34134, Republic of Korea.

[2)]Korea Railroad Research Institute, 176 Cheoldobangmulgwan-ro, Uiwang-si, Gyeonggi-do 16105, Republic of Korea.

[3)]Department of Architectural Engineering, Hanyang University, 222 Wangsimni-ro, Seongdong-gu, Seoul 04763, Republic of Korea.

*Corresponding Author; E-mail: dyyoo@hanyang.ac.kr

Published online: 03 April 2018

strand. They concluded that both minimum concrete cover and clear spacing between prestressing strands in UHPFRC can probably be reduced to 1.5–2.5 times the strand diameter. However, these results were drawn from a limited number of specimens having only one type of $d_p = 12.5$ mm strand embedded in UHPFRC. Hegger and Bertram (2008a) carried out pull-out tests and beam tests to investigate the local bond stress and transfer length, respectively, of prestressing strands embedded in UHPFRC. In their research, UHPFRC had volume fractions of steel fibers varying from 0 to 2.5%, and the effects of varying strand diameters of 0.5–0.6 inches and varying concrete cover depths were investigated. They concluded that the effects of the volume fraction of the steel fibers and the strand diameters on bond behavior between UHPFRC and strands were not significant. However, they found that the effects of the concrete cover depths were dependent on the preset lateral strain of the strands. Moreover, beam tests revealed that the transfer length was extended to about 400–500 mm when the splitting cracks occurred, resulting in a relatively larger transfer length than that without the splitting cracks (about 250 mm). They indicated the need for further tests because the transfer lengths they obtained seemed to be too long. In addition, their study was limited by the compressive strength of UHPFRC used in the study, which was about 100 MPa at the time of testing.

The bond mechanism of a strand is a unique interaction that is characterized by adhesion, Hoyer's effect, and mechanical interlock (Abrishami and Mitchell 1993; Dang et al. 2014), and therefore an understanding of the bond behavior of a strand embedded in UHPFRC should be fully investigated. For this purpose, the research reported in this paper is aimed at providing new test data and demonstrating the effects of the several parameters that affect the bond behavior of prestressing strands in UHPFRC. The pull-out tests were carried out to investigate the factors that affect bond behavior of prestressing strands embedded in UHPFRC, including strand diameter, concrete cover depth, embedment length, and initial prestressing force. Furthermore, beam tests were also conducted using variables similar to those used in the pull-out tests to determine the transfer lengths of strands in UHPFRC. The bond behavior of strands in UHPFRC was compared to that of strands in ordinary high-strength concrete, and the equations for predicting the transfer lengths of strands according to the current code approaches were evaluated with respect to the experimental results.

2. Test Program

2.1 Material Properties

2.1.1 UHPFRC and Steel Fibers

The UHPFRC mix with a target compressive strength of 180 MPa and a target flexural strength of 15 MPa was used in this study; its mix proportions are summarized in Table 1. Type I Portland cement and silica fume were used for the cementitious materials with a water-to-binder ratio (W/B) of 0.2. Based on the packing density theory, silica sand with a grain size less than 0.5 mm was used as the fine aggregate, and silica flour with an average diameter of 2 μm and containing over 98% SiO_2 was used as the filler. Coarse aggregate was excluded from the mixtures in order to improve the homogeneity of the UHPFRC mix.

Straight type micro-steel fibers with a length (l_f) of 13 mm and a diameter (d_f) of 0.2 mm, resulting in an aspect ratio (l_f/d_f) of 65, were added to the UHPFRC mixes up to 2% of the total volume in order to improve the tensile capacity of UHPFRC. These micro-steel fibers are characterized by a density of 7.8 kg/m^3, a tensile strength of 2500 MPa, and an elastic modulus of 200,000 MPa. As significant volumes of cementitious materials and micro steel fibers can result in poor workability of UHPFRC, polycarboxylic acid high-performance water-reducing admixture (superplasticizer) was added to provide proper fluidity.

The mixing sequence for UHPFRC is described elsewhere (Yoo et al. 2014c; Yoo and Yoon 2017). It is noted that this process is different from that of ordinary concrete, as a significantly lower water-to-binder ratio was used and coarse aggregate was excluded from the UHPFRC mix. Fresh concrete properties of UHPFRC, such as air content and flow, were measured before concrete casting, and these results are given in Table 2. The flow of the UHPFRC mix was 167 mm on average, but it ranged from 160 to 170 mm, indicating that enough fluidity was acquired for concrete casting. In order to evaluate the mechanical properties of UHPFRC, three cylindrical specimens ($\phi 100 \times 200$ mm) and three prismatic specimens ($100 \times 100 \times 400$ mm) for each batch were fabricated for compression tests and flexural tests, respectively. These specimens were cured in the following steps: (1) moisture curing at ambient temperature for 24 h prior to form striping; (2) steam curing at a high-temperature of 90 ± 2 °C for 72 h after demolding; and (3) moisture curing at ambient temperature again until mechanical property tests. After the curing process, the compression and flexural tests were carried out in accordance with ASTM C39 (ASTM 2017) and ASTM C1609 (ASTM 2012), respectively, and these results are given in Table 2 as well. The compressive strength of UHPFRC was about 183 MPa with a standard deviation of 8.1 MPa, and the flexural strength of UHPFRC was about 26.7 MPa with a standard deviation of 9.7. Relatively large variations were obtained from the flexural strength, when compared with the compressive strength. In particular, the flexural strength of the third batch of UHPFRC was substantially lower than that of others (1st and 2nd batches). This was mainly due to variations in fiber orientation according to the crack surfaces. However, the strengths of all the batches of UHPFRC were higher than the target value of 15 MPa (see Table 2).

2.1.2 Prestressing Strands

Two different types of low-relaxation, seven-wire steel strands with nominal diameters of 12.7 and 15.2 mm were used for prestressing steel in this study. Both strands were categorized as Grade 270 in ASTM A416 (ASTM 2015), indicating a minimum tensile strength of 1860 MPa. The

Table 1 Mix proportions of UHPFRC by relative weight ratios to cement.

W/B	Relative weight ratios to cement						Steel fiber*
	Water	Cement	Silica fume	Silica sand	Silica flour	Superplasticizer	
0.2	0.227	1.0	0.25	1.1	0.3	0.16	2%

W/B water-to-binder ratio.

* Volume percent of steel fiber in a 1 m^3 UHPFRC mix.

Table 2 Properties of UHPFRC.

Test	Fresh concrete		Hardened concrete	
	Air content (%)	Flow (mm)	Compressive strength (MPa)	Flexural strength (MPa)
1st	2.0	170.0	192.6	34.7
2nd	1.6	170.0	179.6	29.5
3rd	1.0	160.0	177.7	15.9
Average	1.5	166.7	183.3	26.7
STDEV	0.5	5.8	8.1	9.7

Test results presented in a random order, indicating that the results in the same row are not obtained from the same batch of concrete.
STDEV standard deviation.

prestressing strand with a diameter of 12.7 mm, well-known as the standard half inch strand, had a nominal area of 98.7 mm^2, a tensile load of 184 kN, a yield load of 157 kN, and a weight per unit meter of 0.78 kg (or 780 kg/1000 m). The prestressing strand with a diameter of 15.2 mm (0.6 inch strand) had a nominal area of 140 mm^2, a tensile load of 261 kN, a yield load of 222 kN, and a weight per unit meter of 1.1 kg (or 1100 kg/1000 m). Both strands had a modulus of elasticity that ranged from 185 to 205 GPa, a minimum elongation of 3.5%, and a maximum relaxation of 2.5%. The characteristics of the prestressing strands were specified by the manufacturer, and the details are given in Table 3.

2.2 Test Specimen, Setup and Procedure

2.2.1 Bond Strength

The pull-out test was carried out according to the RILEM (1994) recommendation for steel reinforcement (Yuan and Graybeal 2015) to evaluate the bond behavior of prestressing strands embedded in UHPFRC. The primary variables for the pull-out test included the strand diameter (d_b), initial prestressing force (f_{po}), cover concrete depth (c) or cover depth to strand diameter ratio (c/d_b), and embedment length (l_e) in UHPFRC. The compressive strength of UHPFRC was kept constant for all specimens. Two types of strands with diameters of 12.7 and 15.2 mm were considered as the main variables of the experiment. It is noted that shorter embedment lengths, 1 and 2 times the strand diameter ($l_e = 1d_b$ and $2d_b$), than those of the RILEM (1994) recommendation ($l_e = 5d_b$) were used in this study owing to the extremely high-bond strength of UHPFRC (Yoo et al. 2014a). The concrete cover depths of 1–2 times the strand diameter were applied in order to investigate the cover depth effect on the bond strength. Test variables and specimen details for the pull-out tests are summarized in Table 4 and Fig. 1, respectively, as well as in previous research (Kook 2010). All of the pull-out test specimens had the same geometry, which was a 150 mm cubic mold. The fabrications of the pull-test specimens were carried out according to the following steps:

(1) The strands with diameters of 12.7 and 15.2 mm were tensioned at an initial force level, f_{po}, in the pretensioning bed. Each strand having the same diameter was pretensioned in the bed with 80 and 90% of f_{py}, respectively.
(2) Wood forms with dimensions of 150 mm^3 were installed around the strands with varying concrete cover depths ($c = 1d_b$ and $2d_b$) and varying embedment lengths, i.e., 1 and 2 times the strand diameter ($l_e = 1d_b$ and $2d_b$). The unbonded region of the strand, except for embedment length, was covered with a plastic pipe as shown in Fig. 1a.
(3) UHPFRC was cast around the pretensioned strand and cured at ambient temperature for 24 h. Then, it was steam cured at a high-temperature of 90 ± 2 °C for

Table 3 Properties of prestressing strands.

Nom. diameter (mm)	Nom. area (mm^2)	Tensile load (kN)	Yield load (kN)	Weight (kg/1000 m)	Modulus of elasticity (GPa)	Elongation (%)	Relaxation (%)
12.7	98.7	184	157	780	185–205	3.5	2.5
15.2	140.0	261	222	1100	185–205	3.5	2.5

Table 4 Details of specimens for pull-out tests.

Specimen	Strand diameter (mm)	Prestressing force ($\times f_{py}$)	Embedment length (n $\times d_b$)	Cover depth (n $\times d_b$)
13-a-11	12.7	0.8 f_{py}	1 d_s	1 d_s
13-a-12			1 d_s	2 d_s
13-a-22			2 d_s	2 d_s
13-a-2C			2 d_s	5.4 d_s
13-b-11		0.9 f_{py}	1 d_s	1 d_s
13-b-12			1 d_s	2 d_s
13-b-22			2 d_s	2 d_s
15-a-11	15.2	0.8 f_{py}	1 d_s	1 d_s
15-a-12			1 d_s	2 d_s
15-a-22			2 d_s	2 d_s
15-a-2C			2 d_s	4.4 d_s
15-b-11		0.9 f_{py}	1 d_s	1 d_s
15-b-12			1 d_s	2 d_s
15-b-22			2 d_s	2 d_s

a 0.8f_{py}, *b* 0.9f_{py}, *C* center, f_{py} yield strength of strand, d_s diameter of strand.

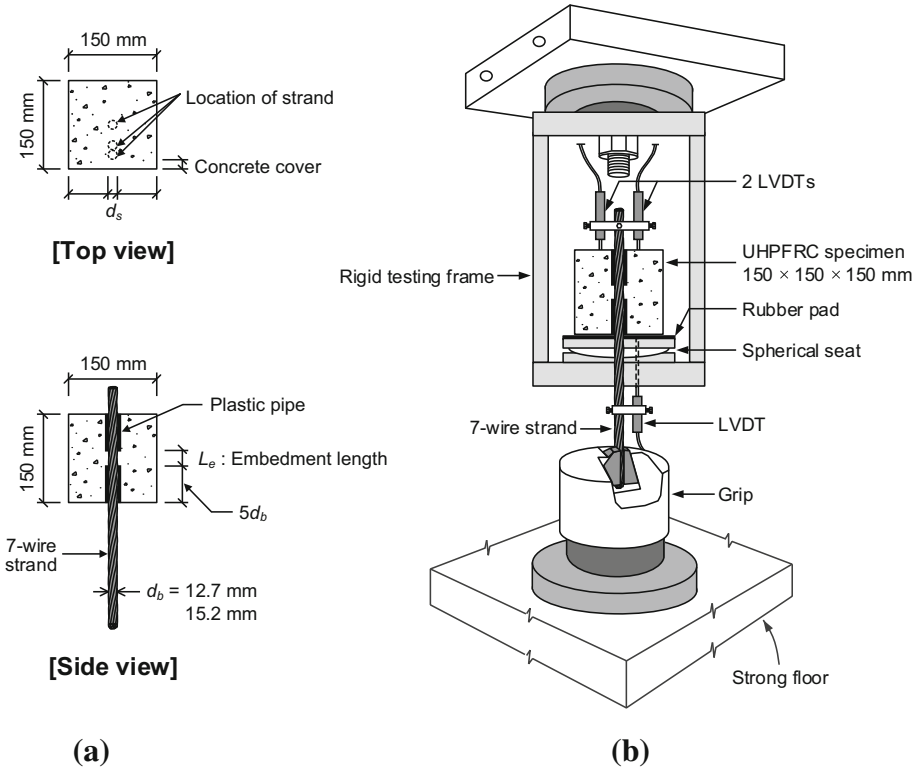

Fig. 1 Pull-out test specimen and test setup; **a** test specimen and **b** test setup.

72 h. It is obvious that the bond strength of strand is strongly affected by the fiber concentration and alignment at near the interface between the strands and UHPFRC. Thus, in order to minimize those effects, UHPFRC was cast identical for all of the specimens in the vertical direction of the strand alignment.

(4) After UHPFRC acquired the desired concrete properties, the strands were released, and the specimens were cured at ambient temperature again before the pull-out tests.

All of the specimens were tested under monotonically increasing pull-out loading with a displacement control rate of 0.3 mm/min. The pull-out load was applied using a 2500 kN capacity computer controlled universal testing machine with a very stiff pull-out test frame (see Fig. 1b). The

specimens with c/d_b of 1 and 2 could experience an eccentric load effect; therefore, a specially fabricated spherical seat and a rubber pad were used between the cubic specimen and the test frame. Two LVDTs were attached at the unloaded (free) end of the strand to measure the average free-end slip, and one LVDT was also attached to the loaded side to determine the yielding of the strand.

Typical jacking stress for low-relaxation strand in the pretensioning bed is $0.75f_{pu}$, which is 75% of ultimate tensile strength of strand (Collins and Mitchell 1991; Zia et al. 1979; Kim et al. 2016). Furthermore, current code provisions limit the maximum stress in prestressed reinforcement as $0.80f_{pu}$ (ACI 318-14 2014; CSA A23.3-14 2014). For low relaxation strand, typical values of f_{py}/f_{pu} is approximately 0.90 (Collins and Mitchell 1991; ASTM A416/A416M), and thus, test variables for initial prestressing forces used in this study, 0.8 and $0.9f_{py}$, were determined to be equivalent to 0.72 and $0.81f_{pu}$, respectively. One of the objectives of this study is to evaluate the effect of initial prestressing force on bond strength of strand embedded in UHPFRC. Test variables for the initial prestressing forces were therefore chosen to cover the aforementioned typical jacking stress ($0.75f_{pu}$) and permissible stress in prestressed reinforcement ($0.80f_{pu}$).

The specimens were marked with the numerals (13 and 15), denoting diameter of strands, and the letters (a or b), denoting initial prestressing with 80 or 90% of f_{py}. The subsequent numerals indicated the multiple of strand diameter for embedment length and cover depth. For example, the 13-a-12 denoted the specimens with 12.7-mm diameter strand, initial prestressing of 80% f_{py}, embedment length of $1d_b$, and cover depth of $2d_b$.

2.2.2 Transfer Length

Six precast, pretensioned concrete beam specimens with a cross section of 150 × 150 mm and a length of 1200 mm were fabricated and tested to evaluate the transfer length of the pretensioning strand. The primary variables were the strand diameter, which included 12.7 and 15.2 mm diameters, and the concrete cover depth, which ranged from 1 to 3 times the strand diameter ($c = 1d_b$ to $3d_b$). The same initial force of 90% of the yield strength of the strand ($f_{po} = 0.9f_{py}$) was applied and the same materials, including UHPFRC and the strand, were also used for all specimens. Test variables for the tests to measure transfer length are summarized in Table 5 and more details are reported elsewhere (Kook 2010).

Details of test specimen and set-up for transfer length measurement are shown in Fig. 2a, while test process is given in Fig. 2b. Strands with diameters 12.7 and 15.2 mm were tensioned at an initial force level, f_{po}, of $0.9f_{py}$ in the pretensioning bed. These strands were instrumented with electrical resistance strain gages to monitor strain variations in the strands. UHPFRC was cast around the strands at varying cover depth to strand diameter ratios, i.e., c/d_b of 1, 2, and 3. The same curing process as that of the pull-out tests was applied to the specimens for the transfer length tests. After the curing process and simultaneous form stripping, electrical resistance strain gages were glued to the side faces of beams at the level of the strands. Then, the strands were released and longitudinal shortenings of the beam specimens were measured to calculate the transfer length.

3. Bond Strengths of Pretensioned Strand in UHPFRC

3.1 Effect of Prestressing Strand Diameter

Figure 3 shows the average bond strengths of prestressing strands in UHPFRC. The average bond strength was calculated by simply assuming a constant bond stress distribution along the embedment length, as follows: $P_{max.}/\pi d_b l_e$, where $P_{max.}$ is the maximum applied load, d_b is the diameter of strand, and l_e is the embedment length. It was obvious that the average bond strength reduced with increasing diameter of the prestressing strand. An approximately 45% higher bond strength on average was obtained in the strands with a smaller diameter compared with those with a larger diameter. This is because a higher pullout force applied to the strand with a larger diameter of 15.2 mm resulted in a more significant decrease in the diameter owing to Poisson's effect; this was not observed for the strand with a smaller diameter of 12.7 mm. A higher pullout force was applied to the strand with a larger diameter than to the strand with a smaller diameter because of its higher bonding area, which was a result of both the higher diameter and embedment length.

Table 5 Test variables and results for beam tests to measure transfer length.

Specimen*	Test variables			Transfer length results	
	Strand diameter (mm)	Prestressing force ($\times f_{py}$)	Cover depth (n × d_b)	Live end (mm)	Dead end (mm)
13-1d_b	12.7	$0.9f_{py}$	1 d_b	237	54
13-2d_b			2 d_b	235	165
13-3d_b			3 d_b	250	242
15-1d_b	15.2	$0.9f_{py}$	1 d_b	380	265
15-2d_b			2 d_b	311	265
15-3d_b			3 d_b	375	246

d_b diameter of strand.

*13 and 15 denote diameter of strands and subsequent #d_b indicates cover depth.

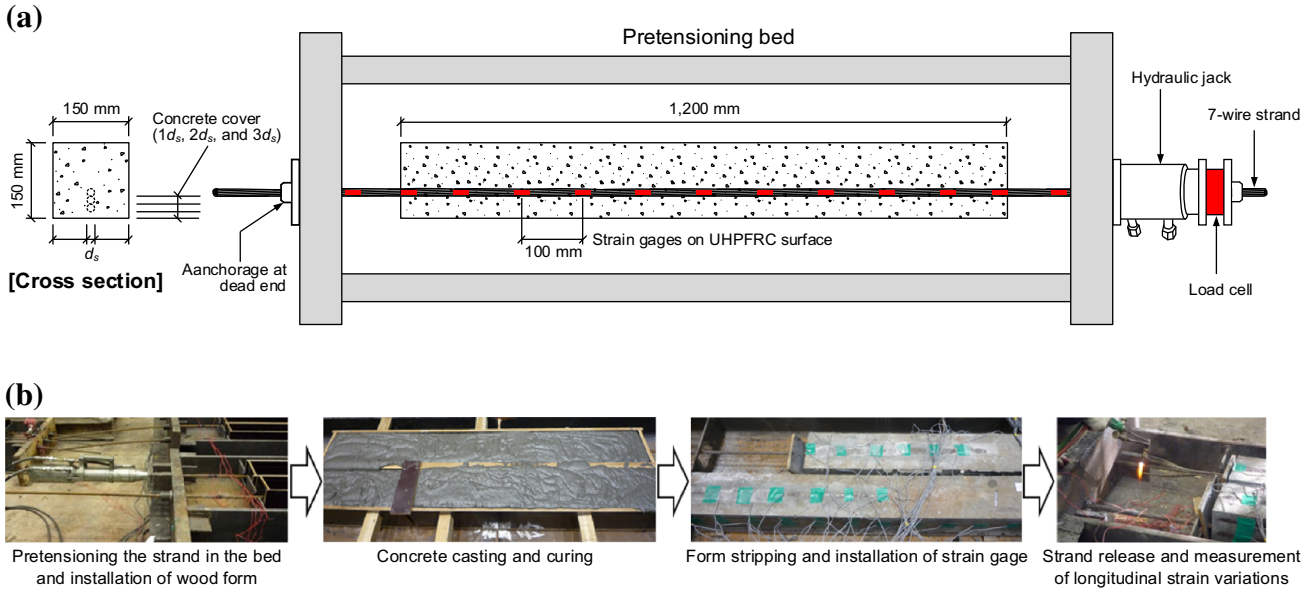

Fig. 2 Test specimen, setup, and procedure for transfer length measurement; **a** test specimen and setup and **b** test procedure.

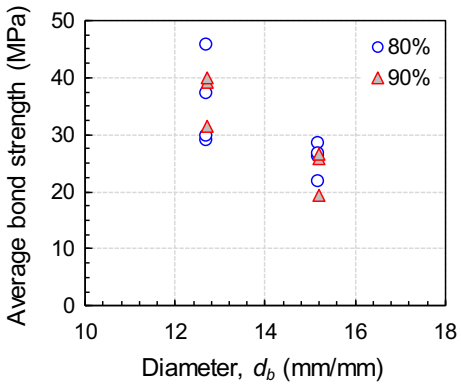

Fig. 3 Effect of diameter on average bond strength.

The higher Poisson's effect led to a decreased confined pressure, and as a result, a lower average bond strength was obtained. Similar observations have already been reported for deformed steel reinforcing bars (Yoo et al. 2015; Yuan and Graybeal 2015) and carbon fiber-reinforced polymer bars (Sayed Ahmad et al. 2011) embedded in UHPFRC.

The highest average bond strength was found to be 45.6 MPa for specimen 13-a-12 (with standard deviation of 7.7), while the lowest bond strength was 19.5 MPa, and it was recorded for specimen 15-b-22 (with standard deviation of 3.9). These values were higher than those of round steel rebar in UHPFRC (Yoo et al. 2014b). For example, the average bond strengths of round steel bars in UHPFRC were found to be 7.0, 6.2, and 5.4 MPa for the cases of $1d_b$, $1.5d_b$, and $2d_b$, respectively. Owing to their deformed shape, which was due to 7-wire twisting and a Hoyer effect at the live end (Hegger et al. 2004), the strands achieved much higher bond strengths than the round steel bars. The diameter of the strand was initially reduced by Poisson's effect when a pretensioning was applied (before cutting the strand). Once cast concrete had achieved a sufficient strength by initial curing, the pretensioned strand was cut, and the pretensioned force was transferred to the concrete as compression. As the strand had a sufficient embedment length, the reduced diameter was maintained owing to the confinement effect of the surrounding concrete. However, the diameter of the strand at the live end was recovered before pretensioning owing to the insufficient embedment length, which caused insufficient confined pressure, and it is called a Hoyer effect. The larger diameter of the strand at the live end acted as an anchor when the prestressing strand was pulled out.

However, the average bond strength of the strands was much smaller than that of the deformed steel rebar in UHPFRC. According to Yoo et al. (2014b), the average bond strengths of deformed steel rebars (d_b of 15.9 mm) embedded in UHPFRC, identical to those used in this study, were obtained as 64.0, 72.0, and 68.8 MPa when the embedded lengths were $1d_b$, $1.5d_b$, and $2d_b$, respectively. Therefore, the bond strengths of prestressing strands in UHPFRC were only approximately 35 and 39% those of deformed steel bars at the embedment lengths of $1d_b$ and $2d_b$, respectively. The main reason for the higher bond strength of deformed steel rebar is the interlocking between the rebar lugs and the surrounding concrete. Owing to this additional mechanical bond component, it is well known that the yielding of a normal-strength steel rebar with f_y of 400 MPa is obtained when the embedment length is equal to or 2 times higher than the rebar diameter ($2d_b$) (Yoo et al. 2014b). Herein, f_y is the yield strength of steel. Therefore, it is concluded that the bond strength of the prestressing strand falls between the bond strengths of round steel and deformed steel rebars.

Girgis and Tuan (2005) have reported that the average bond strength of a 15.2-mm strand in high-strength self-consolidating concrete with a 28-day compressive strength of 55.4 MPa was found to be approximately 9.0 MPa. This indicates that the strand embedded in UHPFRC exhibited much higher bond strength than that embedded in high-strength concrete: the average bond strength of 15.2-mm strand in UHPFRC was found to be 25.0 MPa (with standard deviation of 3.2), approximately 2.8 times higher than that of

the same strand embedded in high-strength concrete. This might be because of an improved strength at the interface between the strand and cement matrix by the filling effect (Yoo et al. 2016c), a significant early age shrinkage development, which caused large lateral confinement (Yoo et al. 2014b) and a limited crack propagation in the steel fibers.

3.2 Effect of Cover Depth to Diameter Ratio (c/d_b)

The bond performance of the prestressing strand is strongly influenced by the failure mode, i.e., pullout failure or splitting failure. The splitting failure will be generated when the circumferential stress at the interface between the stand and cement matrix exceeds the tensile strength. As the bond splitting strength is a function of cover depth to diameter ratio, c/d_b (Rostasy and Hartwich 1988), it is important to investigate the effect of c/d_b ratio on the bond strength of the strand. Furthermore, several researchers (Orangun et al. 1977; Harajli et al. 2002) have reported that the bond strength increases with increasing c/d_b ratio. Thus, the effect of c/d_b ratio on the average bond strength of strands in UHPFRC was examined in Fig. 4. The bond strength of strands in UHPFRC seems to be increased with an increasing c/d_b ratio, which is consistent with the findings of Yuan and Graybeal (2015) for the deformed steel bars in UHPFRC. For example, approximately 21 $\sim$ 57 and 10 $\sim$ 36% higher bond strengths were obtained by increasing the c/d_b ratio from 1 to 2 for the strands with diameters 12.7 and 15.2 mm, respectively. Harajli et al. (2002) reported that the splitting bond strength of a deformed steel bar embedded in ordinary concrete increases with increasing cover depth and amount of fibers. Their (Harajli et al. 2002) results are obvious because the increased concrete cover and fiber amount can effectively prevent the occurrence of splitting cracks in the surrounding concrete. On the other hand, in this study, splitting failure was not visually observed, as shown in Fig. 5, meaning that all the specimens exhibited pullout failure modes regardless of the c/d_b ratio (or cover depth). This might indicate that there must have been micro splitting cracks surrounding UHPFRC even though they were not visible to the naked eye. In addition, in order to quantitatively analyze the effect of c/d_b ratio on the bond strength, p-value was evaluated for the ratios of 1 and 2. The p-value of 0.199 was calculated, which is significantly greater than the threshold value of 0.05, and thus, it is concluded that, although there was a trend of bond strength increase according to the c/d_b ratio (Fig. 4), to draw a certain conclusion on it, further studies with more test data are required.

3.3 Effect of Embedment Length

Figure 6 shows the relationship between the average bond strength and the embedment length of strands in UHPFRC. The average bond strength noticeably decreased with increasing embedment length. The reduced bond strength of deformed steel rebars in UHPFRC was also reported by Yoo et al. (2014b), and several researchers (Abrishami and Mitchell 1996; Hossain 2008) have verified the decrease in bond strength of steel bars with increasing embedment length for ordinary concrete. This is mainly attributed to the fact that the confinement effect of surrounding concrete on the strand is more severely reduced by Poisson's ratio effect when the embedment length increases, because of the increased pullout force. In addition, the nonlinearity in the bond stress distribution along the embedded length increased with increasing embedment length (Abrishami and Mitchell 1996). In other words, the bond stress distribution became more uniform as the embedment length decreased. For this reason, the strand with a shorter embedment length exhibited a higher bond strength than that with a longer length. For example, the average bond strengths of strands with d_b of 12.7 and 15.2 mm reduced by approximately 19 $\sim$ 37 and 6 $\sim$ 27% when the embedment length increased from $1d_b$ to $2d_b$, respectively. More significant decreases in the bond strength with increasing embedment length were observed for the smaller sized strands.

3.4 Effect of Initial Prestressing Force

In order to investigate the effect of the initial prestressing force on the bond strength, two different initial prestressing forces, i.e., 80 and 90% of the yield strength of the strand, were applied. The test results are given in Fig. 7. For both prestressing forces, negligible changes in bond strength were observed. This is inconsistent with the findings of Hegger and Bertram (2008a) that obvious decreases in the bond strength of strands in UHPFRC are observed as the release

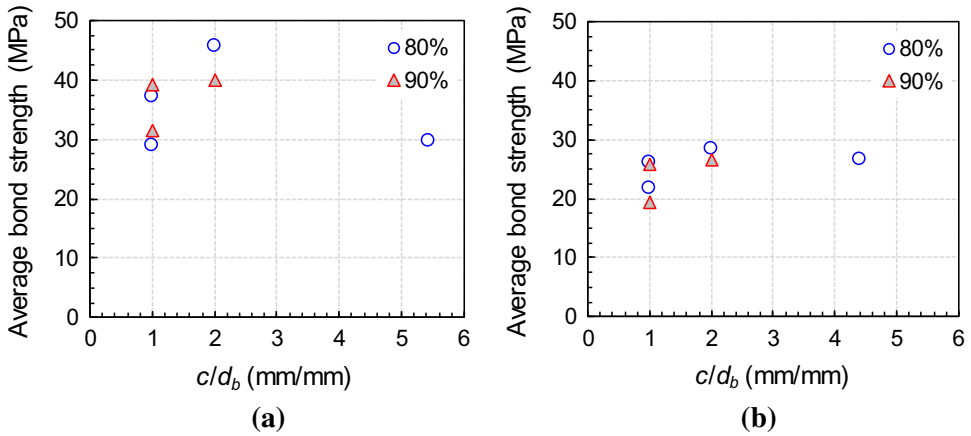

Fig. 4 Effect of cover depth on average bond strength; **a** $l_e = 1d_b$ and **b** $l_e = 2d_b$.

Fig. 5 Pictures for pullout test specimens after complete testing; **a** $c = 1d_b$, **b** $c = 2d_b$, and **c** $c =$ center.

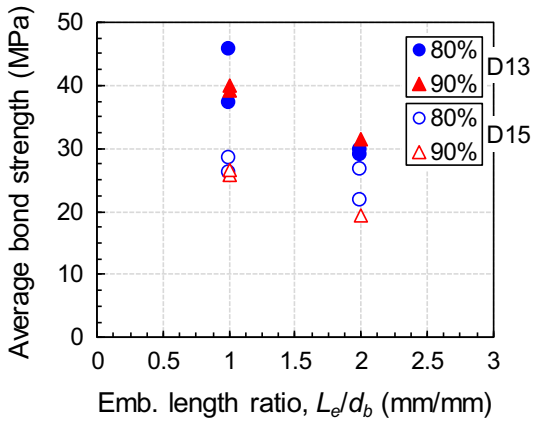

Fig. 6 Effect of embedment length on average bond strength.

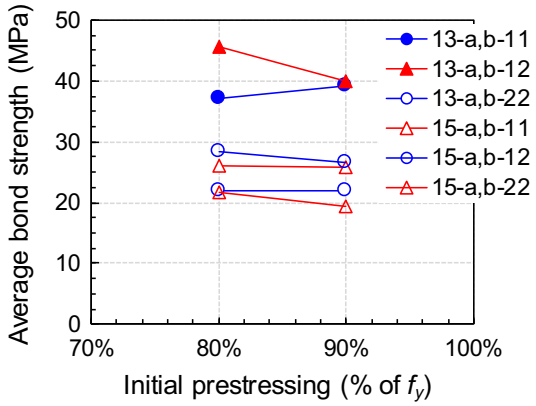

Fig. 7 Effect of initial prestressing magnitude on average bond strength.

percentage of the initial prestressing force is increased, owing to the Hoyer effect. Thus, the negligible change in the bond strength obtained in this study might be due to the small differences between the prestressing forces, which were too small to provide any significant changes for the strands embedded in UHPFRC. In addition, to achieve the significant Hoyer effect required to improve the bond strength of the prestressing strands, a sufficient embedment length is required to transfer strand stress to the surrounding concrete (Hegger et al. 2004). However, in this study, extremely short embedment lengths of $1d_b$ and $2d_b$ that resulted in a limited Hoyer effect were applied. Therefore, it can be comprehensively noted that marginal change in the bond strength of strands in UHPFRC is expected with a slight increase in the initial prestressing force from 80 to 90% of its yield strength when a short embedment length, smaller than the transfer length, is applied.

3.5 Probabilistic Data Analysis

In order to quantify the statistical significance of the relationships between the various parameters (i.e., d_b, L_e, and initial prestressing force) and bond strength, a probability (p)-value was evaluated and analyzed. This probabilistic approach has been adopted by several previous studies (García-Taengua et al. 2014; Zanotti et al. 2018) to precisely evaluate the bond performance of steel-fiber-reinforced concrete (SFRC). It has been well known that a threshold value of p, called a significance level, is traditionally 5%. Based on a bivariate correlations option in a SPSS statistical program, the p-values of 0.12, 1.07, and 97.97% were found for the parameters of d_b, L_e, and initial prestressing force, respectively. This means that only the parameters of diameter (d_b) and embedment length (L_e) significantly affected the bond strength of PS strands embedded in UHPFRC. It is clear that the bond strength of steel reinforcement in SFRC, like UHPFRC, and its interfacial adhesive bond strength are significantly affected by the fiber conditions (i.e., geometry, content, orientation, concentration, etc.) (García-Taengua et al. 2014; Zanotti et al. 2018). The larger p-value was found for the case of parameter L_e than that of d_b. This might be caused by the fact that the larger increase of bonding area leads to the greater variations of bond strength data. In other words, the bond strength of strands in UHPFRC is strongly affected by the fiber alignment and concentration at the interface. Therefore, the increase of bonding area resulted in higher variations of fiber alignment and concentration at the interface, and it caused the higher p-value. The increase of bar diameter from 12.7 mm to 15.2 mm increased the bonding area per unit length of about 20%, while the increase of embedment length from $1 \times d_b$ to $2 \times d_b$ increased the bonding area as much as 100%. However, to more precisely analyze the implication of fiber conditions at the interface on the bond performance, further study is required to be done considering various fiber properties like a previous study (García-Taengua et al. 2014).

4. Transfer Length

The implications of strand diameter and concrete cover depth on the transfer length of UHPFRC were investigated.

Two different strand diameters (12.7 and 15.2 mm) and three different cover depths ($1d_b$, $2d_b$, and $3d_b$) were considered. The strain versus length along the specimen curves are shown in Fig. 8. In order to calculate the transfer length, the 95% average maximum strain (AMS) method, which was introduced by Russell and Burns (1997), was adopted, and the calculated transfer lengths are summarized in Table 5. The following process was used to obtain the transfer length by the 95% AMS method: (1) Draw the strain profile → (2) Determine the average strain value at the strain plateau of the full stress transfer → (3) Draw a straight line based on 95% of the average strain value → (4) Determine the transfer length based on the intersection of the 95% line with the strain profile. For the pretensioning concrete members, a portion of initial prestress is lost immediately after its release due to an elastic shortening phenomenon. Unfortunately, the deformation of concrete members by such an elastic shortening was not measured in the present study, and thus, the elastic shortening was not considered when the transfer length was evaluated. As given in Table 5, it was obvious that the transfer length of the prestressing strand in UHPFRC at the dead end was smaller than that at the live end, regardless of the diameter and cover depth. For example, the transfer lengths at the dead end were approximately 36.7 and 26.5% lower than those at the live end for the strands with diameters of 12.7 and 15.2 mm, respectively. This is consistent with the findings of Russell and Burns (1997) and Kaar et al. (1963) for ordinary concrete without fibers. In particular, according to the test results performed by Russell and Burns (1997), an approximately 34% greater transfer length was obtained at the live end of the 12.7-mm strand than at the dead end, and an about 20% greater transfer length was observed at the live end than at the dead end by Kaar et al. (1963). In addition, the strand with a large diameter of 15.2 mm exhibited higher compressive strains at the concrete surface when exposed to the prestressing force compared with the strand with a lower diameter of 12.7 mm. This is attributed to the fact that a larger prestressing force applied to the strand with a larger size caused a higher compressive strain in the surrounding concrete. Russell and Burns (1997) also reported similar test results for ordinary concrete. John et al. (2011) reported that the transfer length of the prestressing strand in UHPFRC was 355.6 mm (14 in.), and Hegger and Bertram (2008a, b) experimentally obtained transfer lengths that ranged from 250 to 300 mm. Their (Hegger and Bertram 2008a, b) results are similar to the values of transfer lengths obtained in the current study. However, in accordance with Dang et al. (2016a), the transfer length of the strand in high-strength concrete (HSC) with a 28-day compressive strength equal to or higher than 69 MPa ranged from 500 to 730 mm, which was much higher than that of UHPFRC. Thus, it can be noted that prestressing strands embedded in UHPFRC exhibited much shorter transfer lengths compared with those embedded in ordinary HSC.

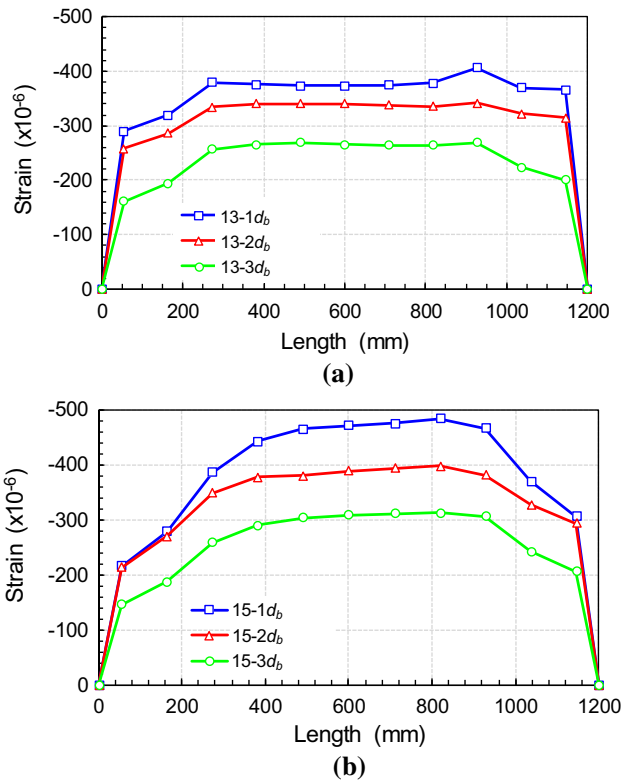

Fig. 8 Strain behaviors along the embedment length for calculating transfer length; **a** d_b of 12.7 mm and **b** d_b of 15.2 mm.

As shown in Fig. 8, higher 95% AMS values were obtained when smaller cover depths were applied for both of the strands with d_b of 12.7 and 15.2 mm. A smaller concrete cover depth resulted in a smaller concrete area surrounding the strand, and as a result, a higher compressive stress was applied to the surrounding concrete at an identical prestressing force. Thus, the higher 95% AMS value was caused by the higher stress generated in the concrete with a smaller cover depth.

The transfer length decreases with increasing compressive strength of concrete (Ramirez-Garcia et al. 2016). This means that the prestressing force is more effectively transferred to the surrounding concrete at shorter embedment length for higher strength concrete, owing to the improved bond performance. Therefore, the applicability of previous equations to predicting the transfer length of prestressing strands embedded in UHPFRC needs to be investigated. Two design codes, i.e., the ACI 318-14 (ACI 2014) and the AASHTO LRFD (AASHTO 2012), which are most widely used, were adopted. The ACI 318 code (ACI 2014) suggests an equation to predict the transfer length of a strand as follows: $L_t = f_{se} \times d_b/20.7$ (in MPa), where L_t is the transfer length, f_{se} is the effective stress in the prestressing strand after losses, and d_b is the strand diameter. In addition, the ACI 318 code (ACI 2014) provides an alternative equation of 50 strand diameters ($50d_b$) for the transfer length, which is effectively used when the parameter f_{se} is unknown, while the AASHTO LRFD code (AASHTO 2012) proposes the transfer length of 60 strand diameters ($60d_b$).

Several other prediction models for transfer lengths of prestressing strands in concrete were also analyzed. Based on a reasonable limit for the higher values of transfer length, Russell and Burns (1996) have proposed the transfer length

Table 6 Comparison of experimental and predicted results.

Spec.*	Exp. result (mm)	Predictive values (mm)								Pred./exp.					
	Live end (1)	ACI 318 (2)	AASHTO LRFD (3)	Russell and Burns (4)	Mitchell et al. (5)	Euro-code 2 (6)	Martí-Vargas et al. (7)	Dang et al. (8)	(2)/(1)	(3)/(1)	(4)/(1)	(5)/(1)	(6)/(1)	(7)/(1)	(8)/(1)
13-1d_b	237	635	762	952	291	240	205	239	2.68	3.22	4.02	1.23	1.01	0.86	1.01
13-2d_b	235								2.70	3.24	4.05	1.24	1.02	0.87	1.02
13-3d_b	250								2.54	3.05	3.81	1.16	0.96	0.82	0.96
15-1d_b	380	760	912	1140	347	286	242	286	2.00	2.40	3.00	0.91	0.75	0.64	0.75
15-2d_b	311								2.44	2.93	3.67	1.12	0.92	0.78	0.92
15-3d_b	375								2.03	2.43	3.04	0.93	0.76	0.65	0.76
Average									2.40	2.88	3.60	1.10	0.90	0.77	0.90
Standard deviation									0.31	0.38	0.47	0.15	0.12	0.10	0.12

d_b diameter of strand.
*13 and 15 denote diameter of strands and subsequent #d_b indicates cover depth.

formula having similar shape with the ACI 318 model, as follows

$$L_t = \frac{f_{se} \times d_b}{13.8} \tag{1}$$

Mitchell et al. (1993) also have suggested a prediction model of transfer length of steel strands embedded in high-strength concrete based on a number of precast, pretensioned concrete beams, as follows

$$L_t = 0.048 f_{pi} d_b \sqrt{\frac{20}{f'_{ci}}}, \tag{2}$$

where f_{pi} is the initial prestressing stress in the strand immediately after a release and f_{ci}' is the initial compressive strength of concrete at the time of release.

Eurocode 2 (EN 2004) have suggested the following equation to predict transfer length of steel strands considering several factors, i.e., tensile strength of concrete, type of strand, surface condition of strand, prestressing force, etc., as follows

$$l_t = \alpha_1 \alpha_2 d_b \frac{f_{pi}}{f_{bpt}}, \tag{3}$$

where α_1 is the coefficient considering the detensioning method (1.0 for gradual release and 1.25 for sudden release), α_2 is the coefficient considering type of strand (0.25 for circular cross section and 0.19 for 3 or 7-wire strand), f_{bpt} is the bond strength between the strand and concrete, given by $f_{bpt} = 2.25\eta_1\eta_2 f_{ctd}$, η_1 is the coefficient regarding bonding condition (1.0 for good bond and 0.7 for all other cases), η_2 equals to 1.0 when strand diameter is smaller than and equal to 32 mm, and f_{ctd} is the design value of concrete tensile strength, $f_{ctd} = \alpha_{ct} f_{ctk,0.05}/\gamma_c$, α_{ct} equals to 1.0, and γ_c equals to 1.5 for persistent load and 1.2 for accidental load, respectively.

Martí-Vargas et al. (2007) have also proposed the following modified formula for transfer length of steel strands in concrete.

$$l_t = \frac{\psi f_{pi} A_{ps}}{(4/3)\pi d_b (0.4)(f'_{ci})^{0.67}} \tag{4}$$

where ψ is a coefficient (= 1) and A_{ps} is the cross sectional area of steel strand.

Lastly, Dang et al. (2016b) have recently suggested the following formulae for transfer length of strands in normal and high-strength self-consolidating concrete, as follows.

$$L_t = \frac{2.63\kappa}{\sqrt{f'_{1d}}} d_b \tag{5}$$

where k is the coefficient (= 96) and f_{1d}' is the compressive strength of concrete at 1 day.

The calculated transfer lengths by three international codes and four prediction models by previous researchers are

summarized in Table 6. It is obvious that the previous ACI 318 and AASHTO LRFD codes significantly overestimate the transfer length of strands embedded in UHPFRC, whereas the Eurocode 2 slightly underestimated it. Similarly, Dang et al. (2016a) reported that the codes overestimated the transfer length of strands embedded in HSC: approximately 1.22–1.78 and 1.47–2.14 times higher transfer lengths were calculated by the ACI 318 and AASHTO LRFD codes, respectively, as compared to the test data. In the case of UHPFRC, the ACI 318 code overestimated the transfer length as 2.14–2.63, while the AASHTO LRFD code overestimated it as 2.57–3.16, which were higher than those for HSC. As UHPFRC provides much improved bond properties when compared with HSC, the ACI 318 and AASHTO LRFD codes further overestimated the actual transfer lengths. The Russell' model most greatly overestimated the transfer length of steel strands in UHPFRC, while the Martí-Vargas's model most greatly underestimated it. The models proposed by Mitchell et al. (1993), Eurocode 2 (EN 2004), and Dang et al. (2016b) quite reasonably predicted the transfer length of strands in UHPFRC with the average ratio (prediction/experiment) of 1.10 and 0.90, respectively. However, for a conservative design perspective, the Mitchell's model could be recommended to be most appropriate for predicting the transfer length of steel strands in UHPFRC.

5. Conclusions

In this study, the bond properties of prestressing strands embedded in UHPFRC were examined. The bond strength of prestressed strands in UHPFRC was evaluated according to the diameter, cover depth, embedment length, and initial prestressing force. In addition, the transfer length of the strands in UHPFRC was estimated based on the 95% AMS method and compared with the predictive values of the ACI 318 and AASHTO LRFD codes. From the above discussion, the following conclusions are drawn:

- The average bond strength of prestressing strands embedded in UHPFRC decreased with increasing strand diameter. The bond strength of strands prestressed by 80 and 90% of the yield strength was higher than that of a round steel rebar, but lower than that of the deformed steel rebar. In addition, the bond strength of the prestressing strand in UHPFRC was approximately 2.8 times higher than that in HSC (f_c' of 55.4 MPa).
- Based on the calculated p-value, only the parameters of bar diameter and embedment length significantly affected the bond strength of strands in UHPFRC.
- A higher average bond strength of the strand in UHPFRC was obtained with smaller bar diameter and embedment length. For the smaller-sized strand, the bond strength was more significantly influenced by the embedment length.
- The average bond strength of the strands was insignificantly affected by the initial prestressing force that ranged from 80 to 90% at short embedment lengths of $1d_b$ and $2d_b$.
- The transfer length of the prestressing strand was shorter at the dead end than at the live end. UHPFRC exhibited much shorter transfer lengths than HSC, and the ACI 318 and AASHTO LRFD codes significantly overestimated the transfer length of a strand embedded in UHPFRC. Based on a design perspective, the model proposed by Mitchell et al. (1993) was considered to be most proper for predicting the transfer length of steel strands in UHPFRCC.

Acknowledgements

This research was supported by a grant from R&D Program of the Korea Railroad Research Institute, Republic of Korea.

References

AASHTO. (2012). *AASHTO LRFD bridge design specifications, Customary U.S. Units* (6th ed.). Washington, DC: American Association of State Highway and Transportation Officials (AASHTO).

Abrishami, H. G., & Mitchell, D. (1993). Bond characteristics of pretensioned strand. *ACI Materials Journal, 90*(3), 228–235.

Abrishami, H. H., & Mitchell, D. (1996). Analysis of bond stress distributions in pullout specimens. *Journal of Structural Engineering, 122*(3), 255–261.

ACI Committee 318. (2014). *Building code requirements for structural concrete (ACI 318-14) and commentary 9 (318R-14)*. Farmington Hills: American Concrete Institute.

ASTM A416. (2015). *Standard specification for low-relaxation, seven-wire steel strand for prestressed concrete* (pp. 1–5). West Conshohocken, PA: ASTM International.

ASTM C1609M. (2012). *Standard test method for flexural performance of fiber-reinforced concrete (using beam with third-point loading)* (pp. 1–9). West Conshohocken, PA: ASTM International.

ASTM C39M. (2017). *Standard test method for compressive strength of cylindrical concrete specimens* (pp. 1–8). West Conshohocken, PA: ASTM International.

BS EN 1992-1-2. (2004). *Eurocode 2: Design of concrete structures Part 1-1: General—common rules for building*

and civil engineering structures. London: British Standards Institution.

Collins, M. P., & Mitchell, D. (1991). *Prestressed concrete structures*. Upper Saddle River, NJ: Prentice Hall.

CSA. (2014). *Design of concrete structures*. Mississauga: Canadian Standards Association.

Dang, C. N., Floyd, R. W., Hale, W. M., & Martí-Vargas, J. R. (2016a). Spacing requirements of 0.7 in. (18 mm) diameter prestressing strands. *PCI Journal, 61*(1), 70–87.

Dang, C. N., Floyd, R. W., Hale, W. M., & Martí-Vargas, J. R. (2016b). Measured transfer lengths of 0.7 in. (17.8 mm) strands for pretensioned beams. *ACI Structural Journal, 113*(1), 85–94.

Dang, C. N., Murray, C. D., Floyd, R. W., Hale, W. M., & Martí-Vargas, J. R. (2014). A correlation of strand surface quality to transfer length. *ACI Structural Journal, 111*(5), 1245–1252.

García-Taengua, E., Martí-Vargas, J. R., & Serna, P. (2014). Splitting of concrete cover in steel fiber reinforced concrete: Semi-empirical modeling and minimum confinement requirements. *Construction and Building Materials, 66,* 743–751.

Girgis, A. F. M., & Tuan, C. Y. (2005). Bond strength and transfer length of pre-tensioned bridge girders cast with self-consolidating concrete. *PCI Journal, 50*(6), 73–87.

Harajli, M., Hamad, B., & Karam, K. (2002). Bond-slip response of reinforcing bars embedded in plain and fiber concrete. *Journal of Materials in Civil Engineering, 14*(6), 503–511.

Hegger, J., & Bertram, G. (2008a). Anchorage behavior of pretensioned strands in steel fiber reinforced UHPC. In *Proceedings of the 2nd International Symposium on Ultra-High Performance Concrete*, Kassel, Germany, pp. 537–544.

Hegger, J., & Bertram, G. (2008b). Shear carrying capacity of steel fiber reinforced UHPC. In *Proceedings of the 2nd International Symposium on Ultra-High Performance Concrete*, Kassel, Germany, pp. 513–520.

Hegger, J., Tuchlinski, D., & Kommer, B. (2004). Bond anchorage behavior and shear capacity of ultra-high performance concrete beam. In *Proceedings of the International Symposium on Ultra High Performance Concrete*, Kassel, Germany, pp. 351–360.

Holschemacher, K., Weiße, D., & Klotz, S. (2004). Bond of reinforcement in ultra high strength concrete. In *Proceedings of the International Symposium on Ultra High Performance Concrete*, Kassel, Germany, pp. 375–388.

Hossain, K. M. A. (2008). Bond characteristics of plain and deformed bars in lightweight pumice concrete. *Construction and Building Materials, 22*(7), 1491–1499.

John, E., Ruiz, E., Floyd, R., & Hale, W. (2011). Transfer and development lengths and prestress losses in ultra-high-performance concrete beams. *Transportation Research Record: Journal of the Transportation Research Board, 2251,* 76–81.

Jungwirth, J., & Muttoni, A. (2004). Structural behavior of tension members in Ultra High Performance Concrete. In *Proceedings of the International Symposium on Ultra High Performance Concrete*, Kassel, Germany, pp. 546–553.

Kaar, P. H., La Fraugh, R. W., & Maas, M. A. (1963). Influence of concrete strength on strand transfer length. *PCI Journal, 8*(5), 47–67.

Kim, J. K., Yang, J. M., & Yim, H. J. (2016). Experimental evaluation of transfer length in pretensioned concrete beams using 2400-MPa prestressed strands. *Journal of Structural Engineering, 142*(11), 04016088.

Kook, K. H. (2010). Crack and bond characteristics of ultra-high-performance concrete for precast segmental cable-stayed bridge [Maters Thesis]. Seoul, South Korea: Korea University.

Martí-Vargas, J. R., Arbeláez, C. A., Serna-Ros, P., Navarro-Gregori, J., & Pallarés-Rubio, L. (2007). Analytical model for transfer length prediction of 13 mm prestressing strand. *Structral Engineering and Mechanics, 26*(2), 211–229.

Mitchell, D., Cook, W. D., Khan, A. A., &Tham, T. (1993). Influence of high strength concrete on transfer and development length of pretensioningstrand. *PCI Journal*, *38*(3), 52–66.

Orangun, C. O., Jirsa, J. O., & Breen, J. E. (1977). A reevaluation of test data on development length and splices. *ACI Journal, 74*(3), 114–122.

Ramirez-Garcia, A. T., Floyd, R. W., Hale, W. M., & Martí-Vargas, J. R. (2016). Effect of concrete compressive strength on transfer length. *Structure, 5,* 131–140.

Richard, P., & Cheyrezy, M. (1995). Composition of reactive powder concretes. *Cement and Concrete Research, 25*(7), 1501–1511.

RILEM TC. (1994). RILEM recommendations for the testing and use of constructions materials. In *RC 6 bond test for reinforcement steel. 2. Pull-out test*. London: E & FN SPON, pp. 218–220.

Rostasy, F. S., & Hartwich, K. (1988). Bond of deformed reinforcing bar embedded in steel fibre reinforced concrete. *International Journal of Cement Composites and Lightweight Concrete, 10*(3), 151–158.

Russell, B. W., & Burns, N. H. (1996). Measured transfer lengths of 0.5 and 0.6 in. strands in pretensioned concrete. *PCI Journal, 41*(5), 44–65.

Russell, B. W., & Burns, N. H. (1997). Measurement of transfer lengths on pretensioned concrete elements. *Journal of Structural Engineering, 123*(5), 541–549.

Sayed Ahmad, F., Foret, G., & Le Roy, R. (2011). Bond between carbon fibre-reinforced polymer (CFRP) bars and ultra high performance fibre reinforced concrete (UHPFRC): Experimental study. *Construction and Building Materials, 25*(2), 479–485.

Yoo, D. Y., Banthia, N., Kang, S. T., & Yoon, Y. S. (2016a). Size effect in ultra-high-performance concrete beams. *Engineering Fracture Mechanics, 157,* 86–106.

Yoo, D. Y., Banthia, N., & Yoon, Y. S. (2016b). Mitigating early-age cracking in thin UHPFRC precast concrete products using shrinkage-reducing admixtures. *PCI Journal, 61*(1), 39–50.

Yoo, D. Y., Kwon, K. Y., Park, J. J., & Yoon, Y. S. (2015). Local bond-slip response of GFRP rebar in ultra-high-

performance fiber-reinforced concrete. *Composite Structures, 120,* 53–64.

Yoo, D. Y., Park, J. J., Kim, S. W., & Yoon, Y. S. (2014a). Influence of reinforcing bar type on autogenous shrinkage stress and bond behavior of ultra high performance fiber reinforced concrete. *Cement & Concrete Composites, 48,* 150–161.

Yoo, D. Y., Park, J. J., Kim, S. W., & Yoon, Y. S. (2014b). Influence of ring size on the restrained shrinkage behavior of ultra high performance fiber reinforced concrete. *Materials and Structures, 47*(7), 1161–1174.

Yoo, D. Y., Shin, H. O., Yang, J. M., & Yoon, Y. S. (2014c). Material and bond properties of ultra high performance fiber reinforced concrete with micro steel fibers. *Composites Part B Engineering, 58,* 122–133.

Yoo, D. Y., & Yoon, Y. S. (2016). A Review on structural behavior, design, and application of ultra-high-performance fiber-reinforced concrete. *International Journal of Concrete Structures and Materials, 10*(2), 125–142.

Yoo, D. Y., & Yoon, Y. S. (2017). Bond behavior of GFRP and steel bars in ultra-high-performance fiber-reinforced concrete. *Advanced Composite Materials, 26*(6), 493–510.

Yuan, J., & Graybeal, B. (2015). Bond of reinforcement in ultra-high-performance concrete. *ACI Structural Journal, 112*(6), 851–860.

Zanotti, C., Rostagno, G., & Tingley, B. (2018). Further evidence of interfacial adhesive bond strength enhancement through fiber reinforcement in repairs. *Construction and Building Materials*. https://doi.org/10.1016/j.conbuildmat.2017.12.140.

Zia, P., Preston, H. K., Scott, N. L., & Workma, E. B. (1979). Estimating prestress losses. *Concrete International, 1*(6), 32–38.